# Electrochemical Reduction of CO 2 Mediated by Quinone Derivatives: Implication for Li–CO 2 Battery

Wei Yin, Alexis Grimaud, Iban Azcarate, Chunzhen Yang, Jean-Marie Tarascon

# Electrochemical Reduction of CO 2 Mediated by Quinone Derivatives: Implication for Li–CO 2 Battery

Wei Yin, Alexis Grimaud, Iban Azcarate, Chunzhen Yang, Jean-Marie Tarascon

# Electrochemical Reduction of $CO_2$ Mediated by Quinone Derivatives: Implication for Li–$CO_2$ Battery

*Wei Yin* [†, ‡], *Alexis Grimaud* [†, §, *], *Iban Azcarate* [†, §], *Chunzhen Yang* [†], *Jean-Marie Tarascon* [†, ‡, §, ∥]

† Chimie du Solide et de l'Energie, FRE 3677, Collège de France, 75231, Paris Cedex 05, France

‡ Sorbonne Universités - UPMC Université Paris 06, Paris, France

§ Réseau sur le Stockage Electrochimique de l'Energie (RS2E), CNRS FR 3459,33 rue Saint Leu, 80039, Amiens Cedex, France

∥ ALISTORE-European Research Institute, Amiens, France

Corresponding author: alexis.grimaud@college-de-france.fr

**Abstract**

The pivotal role of $CO_2$ played in global temperature cycles has motivated the ongoing research on carbon capture and storage (CCS). Within this context, Li─$CO_2$ battery, alike the configuration of Li─$O_2$ battery, has been proposed as a novel energy storage device with the potential to reduce $CO_2$. Nevertheless, the highly negative potential required for the electrochemical reduction of $CO_2$ adds difficulty to the achievement of energy efficient Li─$CO_2$ battery. Facilitating the electron transfer to this inert molecule, which largely dictates the discharge voltage and rate capability of a Li─$CO_2$ battery, is therefore necessary. Herein three types of quinones have been surveyed aiming to mediate the reduction of $CO_2$, which is expected to result in lower overpotential than with a direct electron transfer. We demonstrate by cyclic voltammetry that, in the presence of quinones, $CO_2$ reduction proceeds through an intermolecular interaction between $CO_2$ and quinone dianion. Importantly, such catalytic $CO_2$ reduction reaction is associated with the molecular structure of quinones, the supporting cation (e.g. $Li^+$), and the electrolyte solvent. Furthermore, Li─$CO_2$ battery mediated by 2, 5-di-tert-butyl-1, 4-benzoquinone with $Li_2CO_3$ as the ultimate discharge product is achieved. This study validates the concept of using quinones as chemical catalysts to promote $CO_2$ reduction in Li─$CO_2$ battery. Besides, battery performance and NMR analysis together suggest that side reactions involving quinone itself and/or other cell components occur.

## Introduction

The relentless rise of atmospheric $CO_2$ and the ever-growing energy demands are both critical challenges facing our society. Pursuing renewable energy sources, driven by the needs to increase the energy production without increasing $CO_2$ emissions, motivate the search for efficient energy storage and conversion technologies (e.g. batteries).[1-4] Nevertheless, not only our production of $CO_2$ needs to be decreased, but the atmospheric $CO_2$ concentration must be mitigated back to its pre-industrial level. Various approaches have thus been explored towards this goal, including carbon capture and storage (CCS),[5-6] electrochemical reduction,[7-8] photocatalysis,[9-10] etc. In the context of electrochemical energy storage devices, Li─$CO_2$ battery, alike the configuration of Li─$O_2$ battery, has recently been proposed as a way to transform this detrimental greenhouse gas into value-added energy product like $Li_2CO_3$.[11-12]

In contrast to the $O_2$-based systems, where the electrochemical reduction of $O_2$ into $O_2^{\bullet-}$ in aprotic solvents is thermodynamically more favored (-0.85 V *vs.* SCE in DMF),[13] the reduction of $CO_2$ into $CO_2^{\bullet-}$ requires a highly negative potential (-2.21 V *vs.* SCE in DMF),[14-15] which i) limits the energy efficiency of the battery and ii) induces copious parasitic reactions (e.g. decomposition of the electrolyte solvents that are electrochemically unstable at such potential). Strategies have thus to be envisaged to reduce $CO_2$ with minor side reactions either directly (heterogeneous catalysis) or indirectly (activation reagent or homogeneous catalysis). One example of the latter is provided by introducing $O_2$ into the Li─$CO_2$ system. Consequently, more efficient $CO_2$ reduction is succeeded through an initial electrochemical reduction of $O_2$ to $O_2^{\bullet-}$ which then chemically reacts with $CO_2$ to eventually form $Li_2CO_3$, this system is poised as Li─$O_2$/$CO_2$ battery.[16-18] However, although this approach greatly reduced the energy input requires for the discharge as its potential is now given by the reduction of $O_2$ instead of $CO_2$, the major issue still resides on charge where the oxidation of $Li_2CO_3$ is irreversible, that is, $CO_2$ is released but almost no $O_2$ is given back.[17, 19] Having identified that $O_2$ acts as a scavenger for $CO_2$, Li─$O_2$/$CO_2$ battery is foreseen to be a primary battery.[16-17] Later on, by elevating the battery operation temperature, Archer et al. showed the possibility of direct electrochemical reduction of $CO_2$ in a battery that consumes only $CO_2$ ($4Li + 3CO_2 \rightarrow 2Li_2CO_3 + C$),

the 'real' Li─$CO_2$ battery.[11] But this novel technology still suffers from large overpotential and limited cyclability. Since then, research efforts have been placed in exploring porous carbon based cathode materials (e.g. graphene and carbon nanotube),[20-21] and other heterogeneous electrocatalysts,[12, 22-23] seeking to promote $CO_2$ reduction and/or $Li_2CO_3$ oxidation.

Aside from the battery community, the electrochemical reduction of $CO_2$ in aprotic solvents is also heavily studied by the electrocatalysis community which proposed numerous homogeneous catalysts so to avoid the energy-hungry reaction path, the formation of $CO_2^{\bullet-}$ intermediate, and therefore to improve the kinetics of $CO_2$ reduction.[7, 24] Two types of homogenous catalysts have been described: redox and chemical catalysts. In contrast to redox catalysts for which the catalyst only shuttles the electron from the electrode surface to $CO_2$ following an outer-sphere transfer, chemical catalysts involve $CO_2$ reduction in a chemical step where the catalyst first undergoes electrochemical reduction followed by an adduct formation between the reduced form of the catalyst and $CO_2$, prior to form the final products and to regenerate the parent catalyst.[25-27] Chemical catalysts are attractive options given that they can reduce $CO_2$ with lower activation energy.[24, 26] Similarly, a wide screening for potential redox catalysts (often called "soluble catalyst" or "redox mediator") has been carried out in the Li─$O_2$ field.[28-33] But more interesting is a recent study that demonstrated quinone to operate as the aforementioned chemical catalyst for $O_2$ reduction in Li─$O_2$ battery.[28] In details, once reduced at the electrode surface, quinone diffuses into the electrolyte where it complexes with $Li^+$ and $O_2$ before forming $Li_2O_2$ (the final discharge product). Through such quinone mediated route, the overpotential for $O_2$ reduction could significantly be reduced as it is now controlled by the reduction potential of quinone.

Meanwhile, quinones are well-known for their high binding affinity toward $CO_2$ in their reduced form and have been used to concentrate and selectively separate $CO_2$.[34-36] Furthermore, while a proton source is added in organic solvents so to enhance the kinetics of the $CO_2$ reduction to CO, the synergistic effect of Lewis acid cations such as alkaline cations used in rechargeable batteries (e.g. $Li^+$) on $CO_2$ reduction has also been previously identified.[8, 37]

Altogether, the aforementioned findings decided us to study the possibility of using quinones as chemical catalysts for $CO_2$ reduction to initially form stable quinone─$CO_2$ adducts which, in the presence of alkaline cation (e.g. $Li^+$), could be further reduced to precipitate solid product. We therefore embarked into an in depth electrochemical study to examine this potentiality and further assessed their promises for achieving energy efficient Li─$CO_2$ batteries.

**Experimental Section**

**Chemicals:** N, N-dimethylformamide (DMF, 99.8%, sigma Aldrich), acetonitrile (MeCN, anhydrous, 99.8%, sigma Aldrich), and deuterated acetonitrile ($d_3$-MeCN, ≥ 99.8%, Eurisotop) were dried with activated molecular sieves (4 Å, sigma Aldrich) for at least 2 days before use. Lithium perchlorate ($LiClO_4$, 99.99%, sigma Aldrich), tetrabutylammonium perchlorate ($TBAClO_4$, ≥ 98.0%, sigma Aldrich), 9, 10 anthraquinone (AQ, analytical standard, sigma Aldrich), 9, 10-phenanthrenequinone (PAQ, ≥ 99%, Sigma Aldrich) and 2, 5-di-tert-butyl-1, 4-benzoquinone (DBBQ, 99%, sigma Aldrich) were dried overnight at 80 °C under vacuum in a BÜCHI oven. The water content of the as-prepared electrolytes (solvents and salts) was < 20 ppm as deduced by Karl Fischer titration (Coulometric KF titration, Metrohm). Glass microfiber filters (Whatman) were dried overnight at 220 °C under vacuum in BÜCHI oven.

**Cyclic voltammetry measurements:** A PTFE embedded glassy carbon disk (5.0 mm diam, Pine Research Instrumentation) was used as working electrode, a platinum wire was used as counter electrode. The reference electrode ($Ag^+$/Ag, RE-7, ALS Co., Ltd) consists of a silver wire, a glass tube filled with a MeCN/0.1 M $TBAClO_4$/0.01 M $AgNO_3$ solution (ALS Co., Ltd) and sealed with a Vycor 7930 frit (BioLogic Science Instruments). The reference electrode was assembled in the glovebox at least 24 hours before use and was partially immersed in a MeCN/0.1 M $TBAClO_4$ solution. All measurements were performed in a glove box with water content < 0.5 ppm. The electrochemical cell was well sealed with rubber stoppers except a bubbler which was connected to a gas line that allow to

feed the cell respectively with dry argon (5.0 quality, Linde France) and dry $CO_2$ (5.3 quality, Linde France).

**Cells assembly:** For Li─$CO_2$ cells, two different cell configurations have been used. One is a typical Swagelok cell, the other is a two compartment "Ohara" cell that integrates a ceramic membrane (Lithium ion conductive glass ceramics (LICGC), $Li_{1+x+y}Al_xTi_{2-x}Si_yP_{3-y}O_{12,}$ 200 µm thick, Ohara Inc.) in order to prevent the crossover of quinones. Both of them are integrated with a pressure sensor so to monitor the pressure changes during cell operation, as described elsewhere.[38] All cells were assembled in an argon filled glove box (water content < 1ppm, oxygen content < 1 ppm) with carbon super P positive electrodes and $Li_{1-x}FePO_4$ negative electrodes. The preparation methods of carbon super P and $Li_{1-x}FePO_4$ electrodes are described elsewhere.[17] After assembly, the cells were quickly vacuumed to remove argon inside prior to be filled with $CO_2$ or argon at a constant pressure of 1.55 ± 0.05 bar. Electrochemical behaviors were recorded in a temperature controlled oven with a VMP3 multichannel potentiostat (BioLogic Science Instruments) at a controlled temperature of 25.0 ± 0.05 °C.

**Nuclear magnetic resonance (NMR):** For NMR analyses, deuterated acetonitrile ($d_3$-MeCN) was used as the supporting solvent for the sake of better sensitivity. In order to generate exclusively the reduced form of DBBQ, one cell was discharged in pure argon by first decreasing its potential down to 2 V *vs.* $Li^+$/Li where the reduction takes place, and then hold at this potential until the reduction current gradually decreases close to zero. To differentiate the conditions of electrolyte solutions after the initial electrochemical reduction of DBBQ and the follow-up $CO_2$ chemical reaction, NMR analyses were performed with the solutions collected right after the discharge and after further bubbling with $CO_2$, respectively. All NMR spectra were recorded on a Bruker 300 MHz spectrometer.

## Results and Discussion

Quinones represent a class of organic compounds with versatile physicochemical properties. Among these properties, their redox potentials were found to be dependent on their molecular structures and their chemical environments.[39-41] Therefore, three quinones ─ 9, 10-anthraquinone (AQ), 9, 10-

phenanthrenequinone (PAQ), and 2, 5-di-tert-butyl-1, 4-benzoquinone (DBBQ) ─ have been surveyed in order to select the most suitable one for $CO_2$ reduction in a Li─$CO_2$ battery (Figure 1).

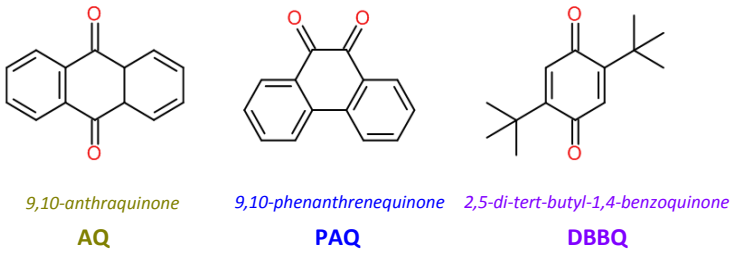


*Figure 1 Chemical structure of the herein investigated quinones*

To spot the electrochemical behavior of quinones in the absence of $CO_2$, voltammetry studies in argon-saturated DMF using tetrabutylammonium ($TBA^+$) as the supporting cation were first conducted. Compared to the voltammograms recorded without quinones where almost no current response was observed (Figure S1a), two well-defined redox waves could be discerned in the presence of quinones, irrespective of their chemical structures (Red lines in Figure 2a). Consistent with previous findings, these two waves correspond successively to the formation/oxidation of quinone anion radicals $Q^{\bullet-}$ and dianions $Q^{2-}$:[36, 42]

$$Q + e^- \leftrightarrow Q^{\bullet-} \qquad (1)$$

$$Q^{\bullet-} + e^- \leftrightarrow Q^{2-} \qquad (2)$$

The reactivity of quinones towards $CO_2$ was then studied, where no substantial change in both the reduction potentials and peak heights for the first reduction waves was observed (Blue lines in Figure 2a), indicating no $CO_2$ reactivity of $Q^{\bullet-}$ independently of the chemistry of quinones. Instead, the second reduction waves are shifted to more positive voltages when adding $CO_2$. Nagaoka et al. reported similar voltammetric behavior and attributed these positive shifts to the coupling of $CO_2$ to $Q^{2-}$ following the reactions:[43]

$$Q + e^- \rightarrow Q^{\bullet-} \qquad (3)$$

$$Q^{\bullet-} + e^- \rightarrow Q^{2-} \qquad (4)$$

$$Q^{2-} + pCO_2 \rightarrow Q(CO_2)_p^{2-} \qquad (5)$$

The reaction of $Q^{2-}$ with $CO_2$ (eqn. (5)) is further confirmed by the disappearance of the $Q^{2-}$ oxidation peak upon $CO_2$ addition, which is typical for an EC mechanism reaction with a fast chemical step.[44]

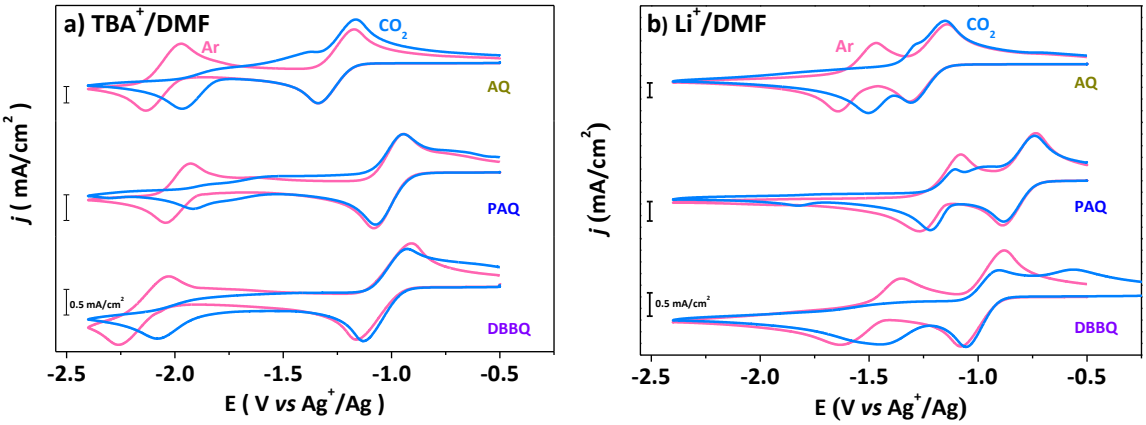


*Figure 2 Cyclic voltammograms of quinones (2.5 mM AQ (top), 5 mM PAQ (middle) and 5 mM DBBQ (bottom)) in Ar- (Red lines) and $CO_2$- (Blue lines) saturated DMF containing 0.1 M $TBAClO_4$ (a), and 0.1 M $LiClO_4$ (b), respectively. Scan rate: 100 mV $s^{-1}$. 2.5 mM AQ was used due to the solubility limit.*

The values of positive shifts measured for the second reduction waves ($\Delta E_2$) following the chemical reactions of $Q^{2-}$ with $CO_2$ (eqn. (5)) are reported in Table S1. As previously established, a higher $\Delta E_2$ value is associated with greater association constant and stoichiometric constant ($p$) for $CO_2$ reaction.[43] Among all the three quinones studied in this work, the highest $\Delta E_2$ value is measured for DBBQ, evidencing its greatest $CO_2$ reactivity which can be partially explained by the better stability of DBBQ─$CO_2$ adduct (the term DBBQ─$CO_2$ adduct was used here for the sake of simplicity, although it was formed from DBBQ dianion and $CO_2$) and its high aromaticity. Similarly, the higher aromaticity of quinone─Li complexes has been demonstrated to favor the $Li^+$ binding.[39] Meanwhile, the fact that $\Delta E_2$ value for PAQ (*ortho*-quinone) was smaller than those for AQ and DBBQ (*para*-quinones) can be related to the steric hindrance, or the coulombic repulsion, induced by the oxygens in *ortho* position for PAQ dianion.

To gain deeper insights into the reaction rate of $Q^{2-}$ and $CO_2$,[44] voltammetry measurements at various sweep rates were performed (Figure S2). Even at a scan rate as high as 20 V $s^{-1}$, no oxidation peak could be recovered for the $Q^{\bullet-} + e^- \rightarrow Q^{2-}$ (eqn. (4)) redox process under $CO_2$, indicating a very fast chemical reaction between $Q^{2-}$ and $CO_2$. Unfortunately, the very fast nature of this step prevents the estimation of its kinetic rate constant.

We then investigated the effects of adding a Lewis acid like $Li^+$ on the reduction of quinones. We should first recall that $Li^+$ was demonstrated, both experimentally and theoretically, to induce positive shifts in the reduction potentials of quinone through the formation of ion-pairs with $Q^{\bullet-}$ and $Q^{2-}$.[45-46] The $Li^+$ association with quinone undoubtedly results in a more complicated system. Therefore we first compared the voltammograms measured under argon with electrolytes containing $Li^+$ and $TBA^+$, as $TBA^+$ does not form stable chelates with organic compounds upon reduction. Similar to what was observed in $TBA^+$–based electrolyte, quinones exhibit successively two reduction waves in the presence of $Li^+$ (Figure S3a). However, when comparing their reduction potentials (Table S2), positive shifts were observed for the first redox waves for DBBQ and PAQ, whereas little change was found for AQ. The difference in the extent of positive shift is related to the different strengths of ion-ion interactions between $Li^+$ and $Q^{\bullet-}$.[45, 47] Indeed, the most pronounced positive shift measured for PAQ is in agreement with its high Li-binding energy, as computationally studied elsewhere.[39] Turning to the second reduction waves, positive shifts were found for all three quinones (Figure S3a). The extent of this shift is in general greater than those for the first waves, suggesting a stronger $Li^+$ association with $Q^{2-}$ than with $Q^{\bullet-}$. Alike what was observed for the first reduction wave, PAQ dianion shows the strongest interaction with $Li^+$ (Table S2). Overall, we have shown that $Li^+$ shifts the reduction potentials of quinones for each electron transfer via ion-ion interactions, following the reactions:

$$Q + e^- + Li^+ \leftrightarrow QLi \qquad (6)$$

$$QLi + e^- + Li^+ \leftrightarrow QLi_2 \qquad (7)$$

Having understood the interaction of $Li^+$ and quinones, we then explored the aforementioned chemical reaction of $CO_2$ with $Q^{2-}$ in the presence of $Li^+$ (Figure 2b). When compared to the results obtained

under argon, the reduction potentials and the peak intensities for the first reduction waves remained unaltered, suggesting that $CO_2$ does not participate in the reduction of quinones upon their initial electron transfer. Nevertheless, positive shifts were found for the second reduction waves for AQ and DBBQ, alike what was observed in $TBA^+$─based electrolytes after $CO_2$ exposure (Figure 2a). After demonstrating that no direct $CO_2$ reduction occurs in the presence of $Li^+$ without quinone (Figure S4a), we can conclude that such positive shifts are indeed related to the chemical reaction of $Q^{2-}$ with $CO_2$. Besides, the disappearance of the oxidation peak of $Q^{2-}$ and the appearance of an oxidation peak at more positive potential (especially in the case of DBBQ) suggested that a new adduct is formed out of the reaction among $Q^{2-}$, $CO_2$ and $Li^+$. Step-wise voltammetry further confirmed that the oxidation peak at more positive potential (i.e. -0.55 V *vs.* $Ag^+$/Ag for DBBQ) is triggered by the formation of quinone─$CO_2$ adduct during the second reduction wave (Figure 3). In contrary, very little change in the voltammogram was observed for PAQ before and after adding $CO_2$, indicating that negligible amount of $CO_2$ reacted with PAQ during reduction (Figure 2b). Such low $CO_2$ affinity for PAQ can be explained by its strong interaction with $Li^+$, as discussed above. In summary, we demonstrated that AQ and DBBQ are capable to react with $Li^+$ and $CO_2$ during their second electron transfer, leading to the formation of a new adduct. Perhaps more importantly, as the reductive currents measured at the end of anodic scan under $CO_2$ and argon were found similar, negligible "surface blocking" effect resulting from the deposition of insulated products formed upon $CO_2$ reduction is expected. This result allow us to conclude that, although $Q^{2-}$ chemically reacts with $CO_2$ and leads to an adduct formation in $Li^+$─based DMF electrolytes, no solid product precipitate out of this reaction. Hence, this reaction is presumably not suitable for designing a Li─$CO_2$ battery with the goal of converting $CO_2$ to a solid product with added value.

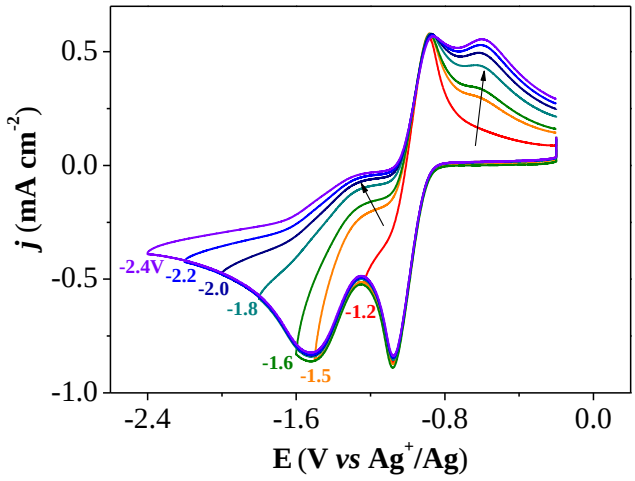


*Figure 3 Stepwise cyclic voltammograms of 5 mM DBBQ in 0.1 M $LiClO_4$/ DMF in the presence of $CO_2$. Scan rate: 100 mV $s^{-1}$.*

In order to tackle the limitation of such $CO_2$ reaction for which no solid product is formed, the solvent was modified. This strategy originates from two observations: i) the redox behavior of quinones was previously demonstrated to be dependent on the solvents[48] and ii) the solubility of the discharge product formed upon $O_2$ reduction in Li─$O_2$ batteries, i.e. $LiO_2$, was shown to correlate with the $Li^+$ solvation strength in different solvents.[49-50] Hence electrochemical results previously collected in DMF were compared to those obtained in MeCN, which is known to have weaker $Li^+$ and stronger anion solvation ability (Table 1), both being defined by the donor number (DN) and acceptor number (AN), respectively.

Table 1 Summary of the intrinsic properties of the herein investigated solvents.

* DN: donor number, AN: acceptor number

| **Solvent** | **DN*** **(Kcal $mol^{-1}$)[51]** | **AN*** **(Kcal $mol^{-1}$)[51]** | **ε** **25 ℃** | **$CO_2$ solubility** **(mM)[52]** | **$10^5$ * $D_{CO2}$** **($cm^2$ $s^{-1}$)[52]** | **Viscosity** **Ƞ (cP)** |
|---|---|---|---|---|---|---|
| **DMF** | 26.6 | 16 | 36.7 | 198 | 3.56±0.2 | 0.92 |
| **MeCN** | 14.1 | 18.9 | 36.64[53] | 280 | 38.3±1.1 | 0.361[53] |

We first considered the influence of the solvents on the reduction of quinone in $TBA^+$–based electrolyte (Figure 4a). A shift towards more positive potentials for the two typical reduction waves for quinone were observed in MeCN (higher AN) when compared to DMF (lower AN) (Table S3). This shift can be explained by the higher AN for MeCN which solvates stronger, and therefore stabilize more, the anions.[54] In $CO_2$–saturated solutions (Blue lines in Figure 4a), little change was found for the reduction potentials and peak intensities for the first reduction waves, but positive shifts were observed for the second reduction waves, revealing the chemical reaction of $Q^{2-}$ with $CO_2$. The positive shifts were in general more pronounced in MeCN than in DMF, indicating a more stable adduct of $Q^{2-}$ and $CO_2$ was formed in MeCN (Table S1). Notably for PAQ and DBBQ, the addition of $CO_2$ causes the disappearance of the oxidation peaks for $Q^{2-}$ and the growth of new oxidation peaks at more positive potentials, suggesting the formation of quinone–$CO_2$ adducts. By comparing the potential of such new oxidation peaks, which can be seen as an indicator of the stability of the quinone–$CO_2$ adducts, DBBQ dianion was determined to exhibit the strongest interaction with $CO_2$ as deduced from its higher oxidation potential. Whereas for AQ, the constant existence of $Q^{2-}$ oxidation peak but situates at a more positive potential implies that the interaction of AQ dianion with $CO_2$ is the weakest.

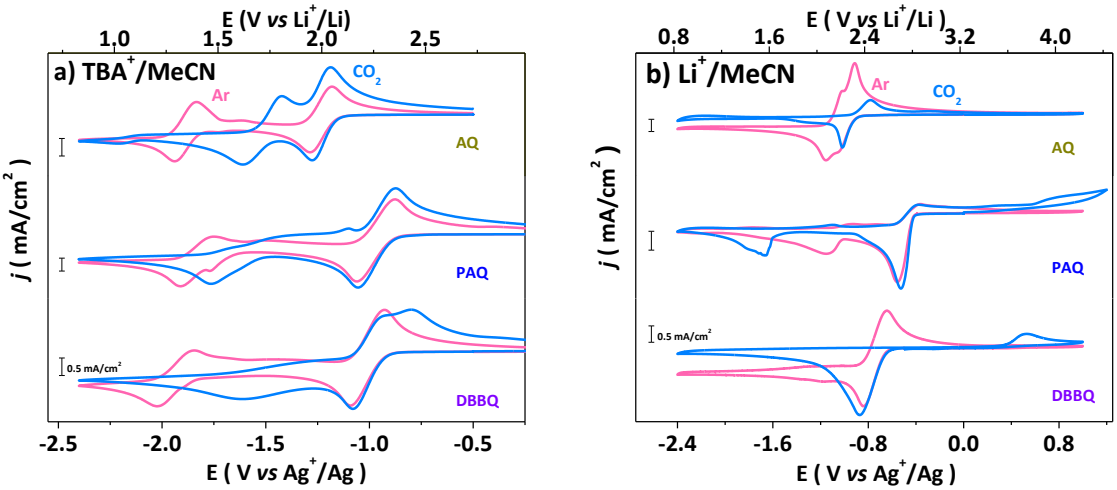


*Figure 4 Cyclic voltammograms of quinones (2.5 mM AQ (top), 5 mM PAQ (middle) and 5 mM DBBQ (bottom)) in Ar- (Red lines) and $CO_2$- (Blue lines) saturated MeCN containing 0.1 M $TBAClO_4$ (a), and 0.1 M $LiClO_4$ (b),respectively. Scan rate: 100 mV $s^{-1}$.*

When comparing our results with those reported previously by Wrighton et al. for PAQ in MeCN/0.1 M $TBABF_4$ solution after the addition of 0.24 M $CO_2$, differences arise. That is, only one redox wave with increased reduction current density was observed in their study, which was interpreted as the change from two successive one-electron processes to a two-electron process in the presence of $CO_2$.[35] However, we found that such variations might result from the presence of water in the electrolyte, as we obtained similar results as in their report when MeCN was not further dried and the water content found relatively high (without drying: 400 ppm (Figure 5a), after drying: < 20 ppm (Figure 5b)). Hence, the presence of water as a proton-source shifts the second reduction wave to a potential identical to that due to the first electron transfer because of the strong interaction of $Q^{2-}$ with proton, i.e. strong H-bonding, as established elsewhere.[55]

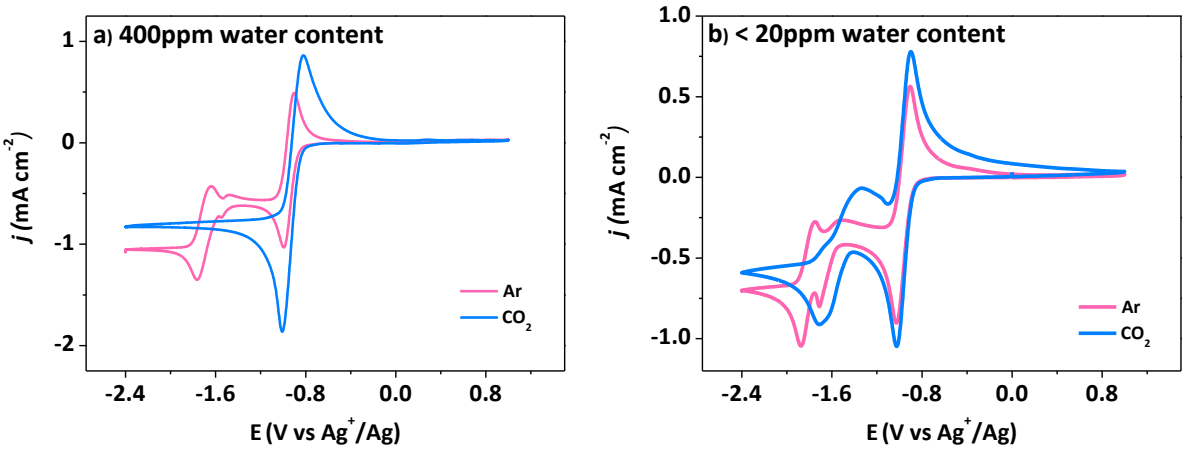


*Figure 5 Cyclic voltammograms of 5 mM PAQ under Ar (Red lines) and $CO_2$ (Blue lines) in MeCN with a water content of 400 ppm (a) and below 20 ppm (b), respectively. Scan rate: 20 mV $s^{-1}$.*

As previously stated, $Li^+$ would shift the reduction waves of quinone toward a positive direction due to its ion association with quinone anions. Obviously, this interaction will itself be modified when modifying the solvation of $Li^+$ by solvent molecules, which follows the DN of solvents.[56] Hence, given the lower DN of MeCN compared to DMF (Table 1), a weaker $Li^+$ solvation strength and thus a stronger $Li^+$ association with quinone anions can already be foreseen. Indeed, we observed in MeCN a greater influence of $Li^+$ on the electrochemical behavior of quinones (green lines in Figure S3b). In contrast to the $Li^+$–based DMF systems where the reduction potentials of quinones shifted to more

positive values while still remaining as two successive waves (green lines in Figure S3a), in the MeCN systems, all quinones lost their typical feature of two well-defined redox waves. More specifically, the second wave for AQ shifted positively to such a large extent that the two redox waves became nearly indistinguishable; only one redox wave at more positive potential was observed for DBBQ; PAQ exhibits two reduction waves but almost no oxidation wave. Hence, in the rest of the study, PAQ will not be further studied. In $CO_2$─saturated electrolytes (blue lines in Figure 4b), little change was observed in terms of the reduction potentials for the first waves, nevertheless, the second reduction waves were consistently pushed toward higher potentials for AQ and DBBQ. Going into more details, the reduction current is found to decrease for AQ, associated with the disappearance of the second reduction peak and the presence of only one oxidation peak at higher voltage than in argon saturated electrolyte. For DBBQ, only one redox peak is observed, presumably arising from the merging of both electron transfers at similar potential. Furthermore, its oxidation peak was shifted at a potential as high as 0.6 V vs. $Ag^+/Ag$ (≈ 3.83 V vs. $Li^+/Li$). Overall, this result suggests a stronger reactivity towards $CO_2$ for DBBQ than for AQ. Moreover, the intensity measured in reduction was found to be almost insensitive to the presence of $CO_2$, suggesting that after its reactivity with $CO_2$ the quinone might not be regenerated. This point will be further developed in the following section. Finally, a typical passivation behavior for which the current drops to zero after the reduction process is observed for DBBQ, as well as for AQ, suggesting the precipitation of a solid product forming an insulating layer on the conductive electrode and which is oxidized at higher potential.

To test the hypothesis that a solid product is precipitated at the end of reduction due to the increased $Li^+$ association and $CO_2$ interaction with quinones in MeCN, Li─$CO_2$ cells were then assembled with MeCN containing either DBBQ or AQ. The overall $CO_2$ pressure was monitored during the cell operation using a Swagelok-derived pressure cell as described elsewhere.[38] In the absence of DBBQ, Li─$CO_2$ cell quickly dies, exhibiting very small discharge capacity (black line in Figure 6a), consistent with the negligible current response previously measured by cyclic voltammetry (Figure S4b). In contrary, Li─$CO_2$ cell with DBBQ discharged under the same condition exhibits a notably greater capacity of ~ 6300 mAh $g^{-1}$ at a discharge plateau of 2.69 V *vs.* $Li^+/Li$ (blue line in Figure 6a). This

discharge plateau is associated with a clear pressure drop (blue line in Figure 6b), confirming that the reduction of DBBQ in $Li^+$─containing MeCN electrolyte is associated with the consumption of $CO_2$. At first glance, our results could naively lead us to conclude that DBBQ significantly promote the discharge in Li─$CO_2$ battery. However, a capacity of ~ 7900 mAh $g^{-1}$ was obtained (red line in Figure 6a) when discharging the cell with DBBQ under argon, which is ~ 36 times higher than the theoretical capacity for the reduction of DBBQ itself ( ~ 216 mAh $g^{-1}$). This discrepancy could be explained by the use of $Li_{1-x}FePO_4$ as anode in these cells (metallic Li cannot be used owing from its reactivity with MeCN). Providing the high redox potential for $Li_{1-x}FePO_4$ (3.45 V *vs.* $Li^+$/Li), the reduced form of DBBQ generated at the cathode upon discharge could diffuse to the anode side where it would be reoxidized. Therefore, to avoid such "shuttle effect" of quinones, a two compartment "Ohara" cell that integrates with a lithium ion conductive glass ceramics was thereby implemented. As expected, a negligible capacity of ~ 34 mAh $g^{-1}$ was obtained in the cell with DBBQ discharging under argon (red line in Figure 6c), indicating that the crossover of DBBQ was effectively avoided. In contrast, a capacity of ~ 160 mAh $g^{-1}$ was achieved when discharging the cell under $CO_2$ (blue line in Figure 6c). A slight pressure drop corresponding to the consumption of $CO_2$ by DBBQ anions was detected (blue line in Figure 6d), while the pressure was found constant in argon cell (red line in Figure 6d). However, the small discharge capacity delivered by this Li─$CO_2$ cell does not allow for a reliable quantification of the amount of $CO_2$ consumed. Nevertheless, we could demonstrate the formation of $Li_2CO_3$ at the end of discharge by XRD (Red line in Figure 7). Accordingly, a high potential (above 4.2 V *vs.* $Li^+$/Li) typically observed for the oxidation of $Li_2CO_3$ was observed on charge (Figure S5). In contrast, for Li─$CO_2$ cell using AQ, a lower discharge voltage associated with a small pressure drop were obtained compared to those measured for DBBQ (Figure 6e and 6f), in agreement with our CV study (Figure 4b), but no crystalline phase could be assigned as the ultimate discharge product by means of XRD (Black line in Figure 7).

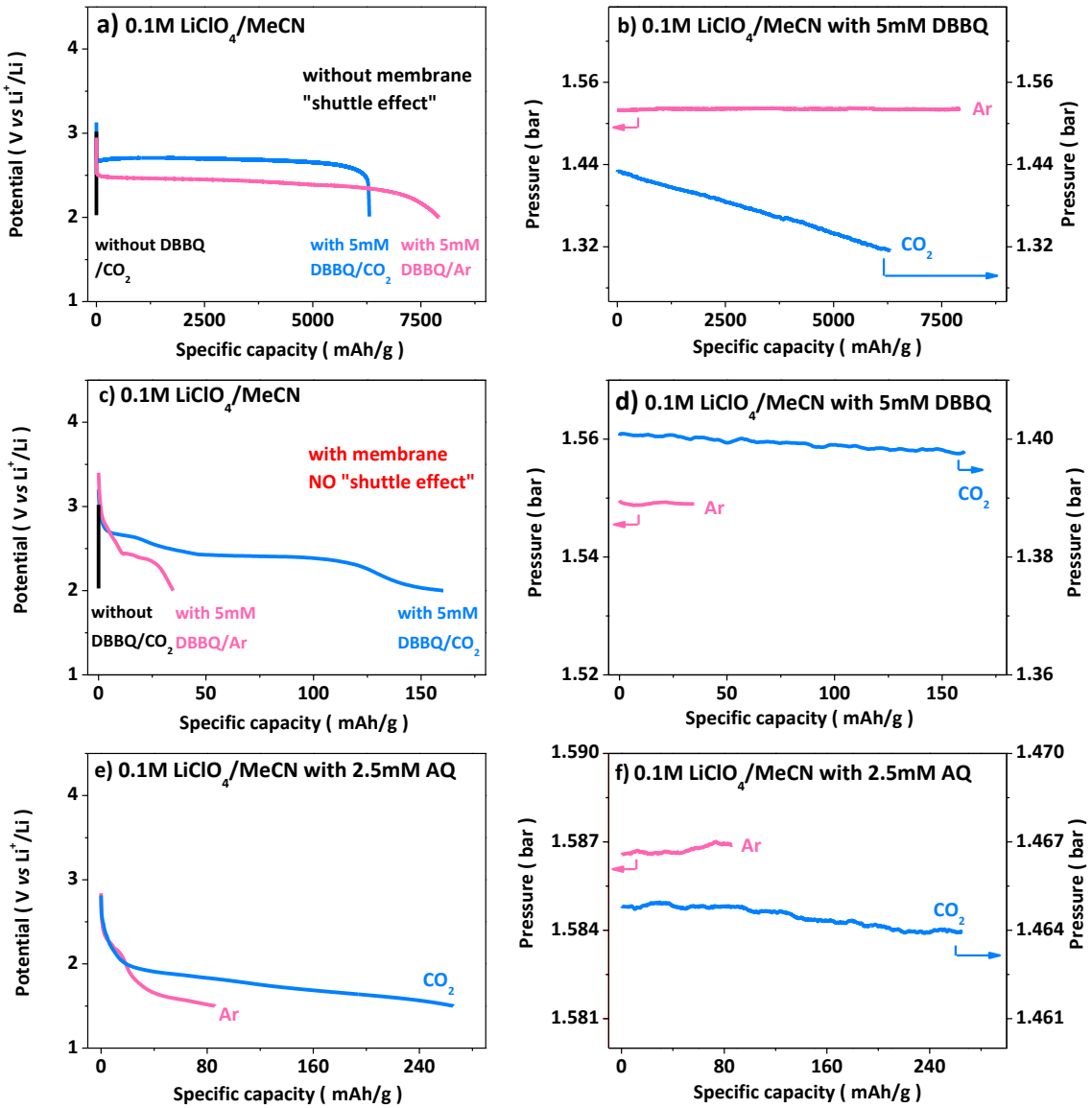


*Figure 6 Galvanostatic discharge curves (a) and pressure changes (b) in 0.1 M $LiClO_4$/MeCN without DBBQ under $CO_2$ (black line), and with 5 mM DBBQ under Ar (Red lines) and $CO_2$ (Blue lines) in a typical pressure cell. Galvanostatic discharge curves (c, e) and pressure changes (d, f) in 0.1 M $LiClO_4$/MeCN with 5 mM DBBQ (c, d) and 2.5 mM AQ (e , f) under Ar (Red lines) and $CO_2$ (Blue lines) in a two-compartment "oraha" cell with a ceramic membrane to prevent the crossover of quinones.*

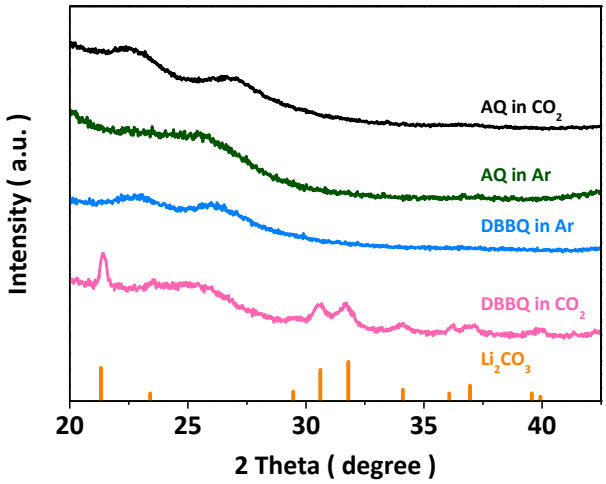


*Figure 7 X-ray diffraction of electrodes after discharged in MeCN with 5mM DBBQ under $CO_2$ (Red line) and Ar (Blue line); and with 2.5 mM AQ under $CO_2$ (Black line) and Ar (Green line). The broad peak at around 26° is referred to carbon Super P.*

Noticing that the discharge capacity obtained from the Li─$CO_2$ cell using DBBQ as a mediator is fairly small, $^1$H NMR was therefore employed to understand i) if soluble products are formed and ii) if degradation of electrolyte or DBBQ occurs upon reduction. Two signals at 6.47 ppm and 1.24 ppm were observed for the solution before discharge, corresponding to the aromatic protons and the protons in the methyl groups of the *tert*-butyl of the unreacted DBBQ, respectively (Figure 8a). After reduction (Figure 8b), two distinct sets of $^1$H NMR signals were detected in the regions of 6.1 - 6.7 ppm (shaded blue and labeled *a*) and 2.8 - 4.5 ppm (shaded grey and labeled *b*). The two peaks in region *a* around the signal for the aromatic protons of DBBQ (6.47 ppm in Figure 8a) can be assigned to the aromatic protons of the reduced form of DBBQ. Nevertheless, one cannot rule out that one of these two signals might arise from the aromatic protons of degradation products arising from the decomposition of DBBQ. The three new peaks in region *b* were not observed in the solution before reduction (Figure 8a), indicating the formation of products with very different proton environment. Although we failed to successfully assign these species using 2D correlation NMR spectroscopy (not shown here), the use of liquid mass spectrometry suggested a quinone degradation mechanism associated with a dimerization phenomenon coupled with the loss of oxygen and tert-butyl groups (Figure S6). Moreover, knowledge from Li─$O_2$ battery can be used to tentatively explain the formation of these peaks. Indeed, redox active electrolyte additives are susceptible to degradation

during battery operation and in some cases can induce degradation of other battery components (e.g. solvents).[30] Hence, bearing in mind that reactive radical species, i.e. DBBQ anion radical, was formed after the initial electron transfer, we can suspect at this stage that these species in region *b* are likely originating from either the degradation of DBBQ itself or the nucleophilic attack of acetonitrile by DBBQ anion radical. Finally, the singlet at 1.31 ppm was assigned to the protons in the methyl groups of the *tert*-butyl group of the reduced DBBQ. Looking into greater details into the peaks at 6.47 ppm and 1.24 ppm which were still present after reduction, one can deduce that a small amount of DBBQ remains unreacted. More importantly, the relative intensity measured for these two peaks clearly increased after bubbling the solution with $CO_2$ (Figure 8c), which can be explained by the regeneration of DBBQ after $CO_2$ reaction, in a manner similar to the $O_2$ reduction mediated by quinone.[28] No extra distinct signal and little change for the three peaks in region *b* were observed after $CO_2$ reaction, likely suggesting that the parasitic degradation is related to the initial electrochemical reduction step. To conclude, NMR analysis revealed the formation of side products during discharge which can possibly explain the limited capacity delivered in DBBQ mediated Li─$CO_2$ battery. This result further emphasizes the importance of the stability for both organic electrolyte solvents and their additives in harsh electrochemical environments for potential Li─gas battery technologies.

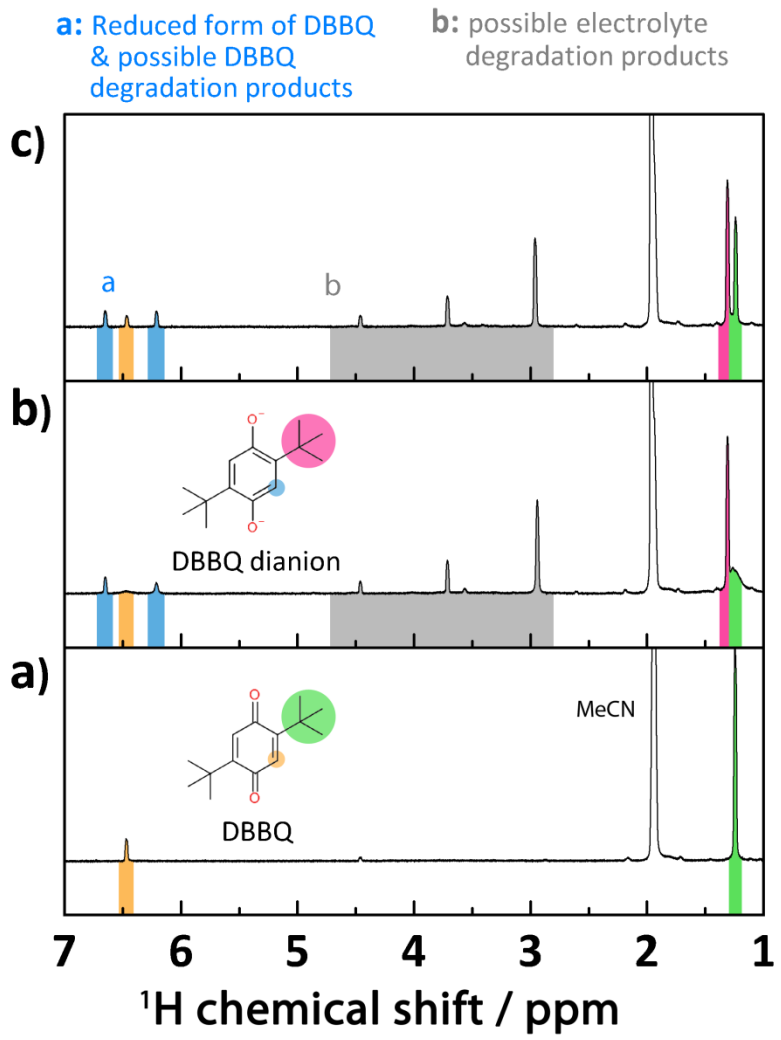


*Figure 8 $^{1}H$ NMR spectra of (a) $d_3$-MeCN + $LiClO_4$ + DBBQ, (b) $d_3$-MeCN + $LiClO_4$ + DBBQ after reduction and (c) $d_3$-MeCN + $LiClO_4$ + DBBQ after reduction and $CO_2$ reaction.*

**Conclusions**

In summary, we first revealed that quinones are capable to reduce $CO_2$ through an intimate chemical interaction between $CO_2$ and quinone anions after their initial electron transfer. The effects of the chemical structure of quinones, the supporting cations (e.g. $Li^+$), and the electrolyte solvents have also been considered. Namely, *para*-quinones interact more intensely with $CO_2$ than *ortho*-quinone. By comparing the voltammograms recorded in electrolytes containing $TBA^+$ and $Li^+$, we found that $Li^+$ might impede the $CO_2$ interactions when a strong ion association between $Li^+$ and quinone anions

occurs. Also, a stronger interaction of $CO_2$ and quinones is observed in MeCN electrolytes when compared to DMF. Furthermore, by adding DBBQ into the electrolyte, the concept of using quinone to mediate $CO_2$ reduction in Li─$CO_2$ battery has been evaluated. The discharge voltage was found to be dictated by the reduction potential of DBBQ. Moreover, $Li_2CO_3$ solid product was identified as the ultimate discharge product. Nevertheless, the limited discharge capacity together with NMR results suggested degradation involving DBBQ itself and/or other cell components. Altogether, our results revealed the complexity of developing Li─$CO_2$ battery with enhanced performances and stability. We believe that despite demonstrating the limitations of using quinones to mediate the formation of $Li_2CO_3$ in aprotic solvents, new strategies can be derived from this work to attain the ambitious goal of converting $CO_2$ into a viable product while delivering energies.

**Supporting Information available**

Additional cyclic voltammetry data, summary of the half-wave reduction potentials obtained under various conditions, galvanostatic discharge-charge curve for DBBQ mediated Li─$CO_2$ battery, and liquid mass spectrometry data.

**Acknowledgment**

The authors would like to thank N. Dubouis, and N. Madern for fruitful discussions as well as G. Gachot for the GC-MS measurements. W.Y. acknowledges a fellowship from the China Scholarship Council (CSC) to perform this work at UPMC and Collège de France.

**Reference**

(1) Larcher, D.; Tarascon, J.-M. Towards Greener and More Sustainable Batteries for Electrical Energy Storage. *Nat. Chem.* **2015,** *7*, 19–29.
(2) Braga, M. H.; Grundisha, N. S.; Murchisona, A. J.; Goodenough, J. B. Alternative Strategy for a Safe Rechargeable Battery. *Energy Environ. Sci.* **2017,** *10*, 331–336.
(3) Bruce, P. G.; Freunberger, S. A.; Hardwick, L. J.; Tarascon, J. M. Li–$O_2$ and Li–S Batteries with High Energy Storage. *Nat. Mater.* **2012,** *11*, 19–29.

(4) Muldoon, J.; Bucur, C. B.; Gregory, T. Quest for Nonaqueous Multivalent Secondary Batteries: Magnesium and Beyond. *Chem. Rev.* **2014,** *114*, 11683–11720.
(5) Wei, J.; Ge, Q.; Yao, R.; Wen, Z.; Fang, C.; Guo, L.; Xu, H.; Sun, J. Directly Converting $CO_2$ into a Gasoline Fuel. *Nat. Commun.* **2017,** *8*, 15174.
(6) Gibbins, J.; Chalmers, H. Carbon Capture and Storage. *Energy Policy* **2008,** *36*, 4317–4322.
(7) Costentin, C.; Robert, M.; Saveant, J. M. Catalysis of the Electrochemical Reduction of Carbon Dioxide. *Chem. Soc. Rev.* **2013,** *42*, 2423–2436.
(8) Bhugun, I.; Lexa, D.; Saveant, J. M. Catalysis of the Electrochemical Reduction of Carbon Dioxide by Iron(0) Porphyrins. Synergistic Effect of Lewis Acid Cations. *J. Phys. Chem.* **1996,** *100*, 19981–19985.
(9) Kuehnel, M. F.; Orchard, K. L.; Dalle, K. E.; Reisner, E. Selective Photocatalytic $CO_2$ Reduction in Water Through Anchoring of a Molecular Ni Catalyst on CdS Nanocrystals. *J. Am. Chem. Soc.* **2017,** *21*, 7217–7223.
(10) Sato, S.; Arai, T.; Morikawa, T. Toward Solar-Driven Photocatalytic $CO_2$ Reduction Using Water as an Electron Donor. *Inorg. Chem.* **2015,** *54*, 5105–5113.
(11) Xu, S.; Das, S. K.; Archer, L. A. The Li–$CO_2$ Battery: A Novel Method for $CO_2$ Capture and Utilization. *RSC Adv.* **2013,** *3*, 6656–6660.
(12) Qiao, Y.; Yi, J.; Wu, S.; Liu, Y.; Yang, S.; He, P.; Zhou, H. Li–$CO_2$ Electrochemistry: A New Strategy for $CO_2$ Fixation and Energy Storage. *Joule* **2017,** *1*, 1–12.
(13) Jain, P. S.; Lal, S. Electrolytic Reduction of Oxygen at Solid Electrodes in Aprotic Solvents–the Superoxide Ion. *Electrochim. Acta* **1982,** *27*, 759–763.
(14) Sullivan, B. P. Electrochemical and Electrocatalytic Reactions of Carbon Dioxide. *Elsevier* **1993**, Laramie,WY,USZ.
(15) Lamy, E.; Nadjo, L.; Saveant, J. M. Standard Potential and Kinetic Parameters of the Electrochemical Reduciton of Carbon Dioxide in Dimethyformamide. *J. Electroanal. Chem.* **1977,** *781977*, 403–407.
(16) Takechi, K.; Shiga, T.; Asaoka, T. A Li–$O_2$/$CO_2$ battery. *Chem. Commun.* **2011,** *47*, 3463–3465.
(17) Yin, W.; Grimaud, A.; Lepoivre, F.; Yang, C.; Tarascon, J.-M. Chemical vs Electrochemical Formation of $Li_2CO_3$ as a Discharge Product in Li–$O_2$/$CO_2$ Batteries by Controlling the Superoxide Intermediate. *J. Phys. Chem. Lett.* **2017,** *8*, 214−222.
(18) Lim, H. K.; Lim, H. D.; Park, K. Y.; Seo, D. H.; Gwon, H.; Hong, J.; Goddard, W. A.; Kim, H.; Kang, K. Toward a Lithium-"Air" Battery: the Effect of $CO_2$ on the Chemistry of a Lithium–Oxygen Cell. *J. Am. Chem. Soc.* **2013,** *135*, 9733–9742.
(19) Yang, S.; He, P.; Zhou, H. Exploring the Electrochemical Reaction Mechanism of Carbonate Oxidation in Li–Air/$CO_2$ Battery Through Tracing Missing Oxygen. *Energy Environ. Sci.* **2016,** *9*, 1650–1654.
(20) Zhang, Z.; Zhang, Q.; Chen, Y.; Bao, J.; Zhou, X.; Xie, Z.; Wei, J.; Zhou, Z. The First Introduction of Graphene to Rechargeable Li–$CO_2$ Batteries. *Angew. Chem., Int. Ed.* **2015,** *54*, 6550–6553.
(21) Zhang, X.; Zhang, Q.; Zhang, Z.; Chen, Y.; Xie, Z.; Wei, J.; Zhou, Z. Rechargeable Li–$CO_2$ Batteries with Carbon Nanotubes as Air Cathodes. *Chem. Commun.* **2015,** *51*, 14636–14639.
(22) Qie, L.; Lin, Y.; Connell, J. W.; Xu, J.; Liming, D. Highly Rechargeable Lithium–$CO_2$ Batteries with a Boron– and Nitrogen–Codoped Holey–Graphene Cathode. *Angew. Chem., Int. Ed.* **2017,** *56*, 6970–6974.
(23) Yang, S.; Qiao, Y.; He, P.; Liu, Y.; Cheng, Z.; Zhu, J.; Zhou, H. A Reversible Lithium–$CO_2$ Battery with Ru Nanoparticles as a Cathode Catalyst. *Energy Environ. Sci.* **2017,** *10*, 972–978.
(24) Savéant, J.-M. Molecular Catalysis of Electrochemical Reactions. Mechanistic Aspects. *Chem. Rev.* **2008,** *208*, 2348–2378.
(25) Andrieux, C. P.; Dumas-Bouchiat, J.-M.; Saveant, J.-M. Homogeneous Redox Catalysis of Electrochemical Reactions: Part I. Introduction. *J. Electroanal. Chem. Interfacial Electrochem.* **1978,** *87*, 39–53.
(26) Bhugun, I.; Lexa, D.; Saveant, J.-M. Ultraefficient Selective Homogeneous Catalysis of the Electrochemical Reduction of Carbon Dioxide by an Iron(0) Porphyrin Associated with a Weak Bronsted Acid Cocatalyst. *J. Am. Chem. Soc.* **1994,** *116*, 5015–5016.

(27) Costentin, C.; Drouet, S.; Robert, M.; Saveant, J.-M. A Local Proton Source Enhances $CO_2$ Electroreduction to CO by a Molecular Fe Catalyst. *Science* **2012,** *338*, 90–94.
(28) Gao, X.; Chen, Y.; Johnson, L.; Bruce, P. G. Promoting Solution Phase Discharge in Li–$O_2$ Batteries Containing Weakly Solvating Electrolyte Solutions. *Nat. Mater*. **2016,** *15*, 882–888.
(29) Chen, Y.; Freunberger, S. A.; Peng, Z.; Fontaine, O.; Bruce, P. G. Charging a Li–$O_2$ Battery Using a Redox Mediator. *Nat. Chem.* **2013,** *5*, 489–494.
(30) McCloskey, B. D.; Addison, D. A Viewpoint on Heterogeneous Electrocatalysis and Redox Mediation in Nonaqueous Li–$O_2$ Batteries. *ACS Catal.* **2017,** *7*, 772–778.
(31) Liang, Z.; Lu, Y. C. Critical Role of Redox Mediator in Suppressing Charging Instabilities of Lithium Oxygen Batteries. *J. Am. Chem. Soc.* **2016,** *138*, 7574–7583.
(32) Sun, D.; Shen, Y.; Zhang, W.; Yu, L.; Yi, Z.; Yin, W.; Wang, D.; Huang, Y.; Wang, J.; Wang, D.; Goodenough, J. B. A Solution-Phase Bifunctional Catalyst for Lithium–Oxygen Batteries. *J. Am. Chem. Soc.* **2014,** *136*, 8941–8946.
(33) Gao, X.; Chen, Y.; Johnson, L. R.; Jovanov, Z. P.; Bruce, P. G. A Rechargeable Lithium–Oxygen Battery with Dual Mediators Stabilizing the Carbon Cathode. *Nat. Energy* **2017,** *2*, 17118.
(34) Rheinhardt, J. H.; Singh, P.; Tarakeshwar, P.; Buttry, D. A. Electrochemical Capture and Release of Carbon Dioxide. *ACS Energy Lett.* **2017,** *2*, 454–461.
(35) Mizen, M. B.; Wrighton, M. S. Reductive Addition of $CO_2$ to 9, 10-Phenanthrenequinone. *J. Electrochem. Soc.* **1989,** *136*, 941–946.
(36) Gurkan, B.; Simeon, F.; Hatton, T. A. Quinone Reduction in Ionic Liquids for Electrochemical $CO_2$ Separation. *ACS Sustainable Chem. Eng.* **2015,** *3*, 1394–1405.
(37) Resasco, J.; Chen, L. D.; Clark, E.; Tsai, C.; Hahn, C.; Jaramillo, T. F.; Chan, K.; Bell, A. T. Promoter Effects of Alkali Metal Cations on the Electrochemical Reduction of Carbon Dioxide. *J. Am. Chem. Soc.* **2017,** *139*, 11277–11287.
(38) Lepoivre, F.; Grimaud, A.; Larcher, D.; Tarascon, J. M. Long-Time and Reliable Gas Monitoring in Li–$O_2$ Batteries via a Swagelok Derived Electrochemical Cell. *J. Electrochem. Soc.* **2016,** *163*, A923–A929.
(39) Ding, Y.; Li, Y.; Yu, G. Exploring Bio-inspired Quinone-Based Organic Redox Flow Batteries: A Combined Experimental and Computational Study. *Chem* **2016,** *1*, 790–801.
(40) Wilfrod, J. H.; Archer, M. D. Solvent Effects on the Redox Potentials of Benzoquinone. *J. Electroanal. Chem.* **1985,** *190*, 271–277.
(41) Neeraj, G.; Henry, L. Hydrogen-Bonding and Protonation Effects in Electrochemistry of Quinones in Aprotic Solvents. *J. Am. Chem. Soc.* **1997,** *119*, 6384–6391.
(42) Guin, P. S.; Das, S.; Mandal, P. C. Electrochemical Reduction of Quinones in Different Media: A Review. *Int. J. Electrochem.* **2011,** *2011*, 1–22.
(43) Tsutomu, N.; Nobuyuki, N.; Koji, F.; Kotaro, O. Mechanisms of Reductive Addition of $CO_2$ to Quinones in Acetonitrile. *J. Electroanal. Chem.* **1992,** *322*, 383–389.
(44) Saveant, J.-M. Elements of Molecular and Biomolecular Electrochemistry. *Wiley* **2006**, Paris, France.
(45) Fujinaga, T.; Izutsu, K.; Nomura, T. Effect of Metal Ions on the Polarographic Reduction of Organic Compounds in Dipolar Aprotic Solvents. *J. Electroanal. Chem.* **1971,** *29*, 203–209.
(46) Kim, K. C.; Liu, T.; Lee, S. W.; Jang, S. S. First-Principles Density Functional Theory Modeling of Li Binding: Thermodynamics and Redox Properties of Quinone Derivatives for Lithium–Ion Batteries. *J. Am. Chem. Soc.* **2016,** *138*, 2374–2382.
(47) Marek, K. K.; Barbara, T. G. Ion-pair Effects in the Electrochemistry of Aromatic Compounds Effects of Metal Ions and Solvents on the Polarographic Reduction of Quinones. *J. Electroana. Chem. Interfacial Electrochem.* **1974,** *55*, 277–286.
(48) Kazuo, S.; Tomoyuki, K.; Masahiro, O.; Yasushi, O.; Nobuaki, O. Solvent Effect in the Electrochemical Reduction of p-Quinones in Several Aprotic Solvents. *J. Electrochem. Soc.* **1990,** *137*, 2437–2443.
(49) Johnson, L.; Li, C.; Liu, Z.; Chen, Y.; Freunberger, S. A.; Ashok, P. C.; Praveen, B. B.; Dholakia, K.; Tarascon, J. M.; Bruce, P. G. The role of $LiO_2$ solubility in $O_2$ reduction in aprotic solvents and its consequences for Li–$O_2$ batteries. *Nat. Chem* **2014,** *6* (12), 1091–1099.

(50) Lutz, L.; Yin, W.; Grimaud, A.; Alves Dalla Corte, D.; Tang, M.; Johnson, L.; Azaceta, E.; Sarou-Kanian, V.; Naylor, A. J.; Hamad, S., et al. High Capacity Na–$O_2$ Batteries: Key Parameters for Solution-Mediated Discharge. *J. Phys. Chem. C* **2016,** *120*, 20068–20076.
(51) Kwabi, D. G.; Bryantsev, V. S.; Batcho, T. P.; Itkis, D. M.; Thompson, C. V.; Shao-Horn, Y. Experimental and Computational Analysis of the Solvent-Dependent $O_2$/Li(+)–$O_2$(–) Redox Couple: Standard Potentials, Coupling Strength, and Implications for Lithium–Oxygen Batteries. *Angew. Chem. Int. Ed* **2016,** *55*, 3129–3134.
(52) Wadhawan, J. D.; Welford, P. J.; McPeak, H. B.; Hahn, C. E. W.; Compton, R. G. The simultaneous voltammetric determination and detection of oxygen and carbon dioxide A study of the kinetics of the reaction between superoxide and carbon dioxide in non-aqueous media using membrane-free gold disc microelectrodes. *Sens Actuators B* **2003,** *88*, 40–52.
(53) Laoire, C. O.; Mukerjee, S.; Abraham, K. M.; Plichta, E. J.; Hendrickson, M. A. Influence of Nonaqueous Solvents on the Electrochemistry of Oxygen in the Rechargeable Lithium−Air Battery. *J. Phys. Chem. C* **2010,** *114*, 9178–9186.
(54) Jaworski, J. S.; Lesniewska, E.; Kalinowski, M. K. Solvent Effect on the Redox Potential of Quinone-Semiquinone Systems. *J. Electroanal. Chem.* **1979,** *105*, 329–334.
(55) Staley, P. A. The Electrochemistry of Quinones in Aprotic Solvents. *Ph.D. Thesis* **December 2016**, University of California, San Diego, San Diego State University.
(56) Burger, K. Solvation, Ionic and Complex Formation Reactions in Non-Aqeuous Solvents. *Elsevier Science* **1983**, Budapest, Hungary.

**TOC Graphics**